Diabetes, Metabolic Syndrome and Obesity

Dovepress

open access to scientific and medical research

Open Access Full Text Article

ORIGINAL RESEARCH

Aberrant Neurovascular Coupling in Diabetic Retinopathy Using Arterial Spin Labeling (ASL) and Functional Magnetic Resonance Imaging (fMRI) methods

Yu-Lin Zhong[1,*], Rui-Yang Hu[2,*], Xin Huang[1]

[1]Department of Ophthalmology, Jiangxi Provincial People's Hospital, The First Affiliated Hospital of Nanchang Medical College, Nanchang, Jiangxi, 330006, People's Republic of China; [2]School of Ophthalmology and Optometry, Jiangxi Medical College, Nanchang University, Nanchang, Jiangxi, 330006, People's Republic of China

*These authors contributed equally to this work

Correspondence: Xin Huang, Department of Ophthalmology, Jiangxi Provincial People's Hospital, No. 152, Ai Guo Road, Dong Hu District, Nanchang, Jiangxi, 330006, People's Republic of China, Tel +86 15879215294, Email 334966891@qq.com

Background: Previous imaging studies have demonstrated that diabetic retinopathy (DR) is linked to structural and functional abnormalities in the brain. However, the extent to which DR patients exhibit abnormal neurovascular coupling remains largely unknown.

Methods: Thirty-one patients with DR and 31 sex- and age-matched healthy controls underwent resting-state functional magnetic resonance imaging (rs-fMRI) to calculate functional connectivity strength (FCS) and arterial spin-labeling imaging (ASL) to calculate cerebral blood flow (CBF). The study compared CBF-FCS coupling across the entire grey matter and CBF/FCS ratios (representing blood supply per unit of connectivity strength) per voxel between the two groups. Additionally, a support vector machine (SVM) method was employed to differentiate between diabetic retinopathy (DR) patients and healthy controls (HC).

Results: In DRpatients compared to healthy controls, there was a reduction in CBF-FCS coupling across the entire grey matter. Specifically, DR patients exhibited elevated CBF/FCS ratios primarily in the primary visual cortex, including the right calcarine fissure and surrounding cortex. On the other hand, reduced CBF/FCS ratios were mainly observed in premotor and supplementary motor areas, including the left middle frontal gyrus.

Conclusion: An elevated CBF/FCS ratio suggests that patients with DR may have a reduced volume of gray matter in the brain. A decrease in its ratio indicates a decrease in regional CBF in patients with DR. These findings suggest that neurovascular decoupling in the visual cortex, as well as in the supplementary motor and frontal gyrus, may represent a neuropathological mechanism in diabetic retinopathy.

Keywords: neurovascular coupling, diabetic retinopathy, arterial spin labelling, cerebral blood flow, functional connectivity strength, resting-state, SVM

Introduction

Diabetic retinopathy (DR) is the prevailing microvascular complication of diabetes mellitus and a crucial risk factor for vision impairment in patients with diabetes.[1] The observation of diabetic maculopathy can be credited to Eduard Jaeger in 1856.[2] According to a 2020 survey, the global prevalence of DR among individuals with diabetes stood at 22.27%, affecting approximately 103.12 million people worldwide. This number is projected to rise to 160.5 million by 2045, with the highest prevalence recorded in Africa at 35.90%, closely followed by North America at 33.30%.[3] It is evident that, in addition to technological limitations, the prevalence of diabetic retinopathy remains substantial among diabetic patients. This emphasizes the critical need for support in diagnosing diabetic retinopathy and initiating early treatment through various techniques,

Received: 2 April 2024
Accepted: 7 July 2024
Published: 26 July 2024

including imaging.[4] The primary pathological changes in diabetic retinopathy typically commence with microaneurysms and advance to exudative lesions. Previous studies have demonstrated that patients with diabetic retinopathy have a higher risk of Alzheimer's disease and dementia, which may be closely related to cognitive decline [5–7] The findings of S Busiguina et al on the association of neurodegeneration with insulin-like growth factor provide further confirmation of previous inferences.[8] And it is likely that diabetic retinopathy, one of the more common microvascular complications of diabetes, also has abnormal neurovascular function. Exploring the abnormal alterations in neurovascular coupling function in patients with diabetic retinopathy provides an imaging reference for future investigation of the mechanisms of injury.

CBF is the volume of blood that reaches a specific mass of brain tissue within a defined time period. It is intricately linked to brain tissue metabolism, encompassing processes such as glucose utilization, aerobic glycolysis, and oxygen consumption.[9] Positron emission tomography (PET) and single photon emission computed tomography (SPECT) have been extensively employed for detecting CBF abnormalities in patients with DR.[10,11] However, both PET and SPECT techniques are invasive, involve long acquisition times, and offer limited spatial resolution. Conversely, arterial spin labeling (ASL) magnetic resonance imaging is a non-invasive method that enables quick quantification of CBF using endogenous contrast.[12,13] This technique has been previously utilized to investigate patients with type 2 diabetes mellitus, revealing significantly lower regional cerebral blood flow (rCBF) values in the bilateral frontal lobe, cingulate gyrus, medial temporal lobe, thalamus, and right occipital lobe compared to controls.[14] We also conducted this study on patients with DR, which revealed significantly higher CBF values in the left middle temporal gyrus and bilateral supplementary motor areas, as well as significantly lower CBF values in the bilateral calyces and bilateral caudate nuclei.[15]

Resting-state functional connectivity (rsFC) assesses the temporal correlation of low-frequency fluctuations in blood oxygen level-dependent (BOLD) signals across different brain regions.[16] Low-frequency BOLD signals are vulnerable to physiological processes like respiration and cardiac oscillations, potentially causing unreliable outcomes when utilizing the rsFC method.[17] Conversely, seed-based FC methods necessitate prior knowledge of the seed region.[18] Functional connectivity strength (FCS) analysis is an innovative data-driven approach that quantifies mean FC by assessing the correlation between each voxel and all other voxels throughout the brain.[19] Brain regions characterized by high Functional Connectivity Strength (FCS) are recognized as functional hubs, exhibiting elevated connectivity with the broader brain network. We have previously employed independent component analysis(ICA) technique in patients with DR and observed abnormal large-scale functional network changes in DR patients.[20]

The human brain comprises approximately 20% of the body's total energy demands. Its metabolic processes predominantly utilize glucose to generate energy, crucial for sustaining spontaneous brain activity.[21,22] Under the coupled neuro-vascular hypothesis, brain regions exhibiting higher neuronal activity are thought to be more metabolically proficient, resulting in elevated perfusion.[23,24] Concurrently, the intensity of neuronal activity in a brain region mirrors the extent of its functional connectivity with other brain regions.[25] Neurovascular coupling is an important mechanism to ensure adequate blood supply to active neurons in the brain.The CBF/FCS ratio quantifies the blood supply per unit of connectivity strength, depicting the neurovascular coupling of a specific voxel or region.[19] Ruan et al demonstrated that patients with vascular cognitive impairment (VCI) exhibited diminished neurovascular coupling at the whole-brain level compared to healthy controls (HCs).[26] Shang et al reported global and regional cerebral blood flow-ReHo decoupling in Parkinson's disease. The CBF/ReHo ratio features yielded superior classification performance compared to other features.[27] The CBF/FCS method offers several advantages. Firstly, it is a non-invasive technology that does not require the use of contrast agents during fMRI scanning. Secondly, the CBF/FCS method provides high spatial resolution and can accurately reflect neurovascular coupling signals in the brain. Therefore, the CBF/FCS ratio can serve as a valuable tool for identifying alterations in neurovascular coupling among patients with diabetic retinopathy (DR) that may not be discernible through the examination of CBF and FCS individually. Our study solely utilized multimodal magnetic resonance imaging to compare patients with DR and healthy individuals. However, it did not conduct a longitudinal assessment of the imaging alterations associated with neurovascular coupling in DR patients. Currently, there is a lack of studies investigating the abnormal neurovascular coupling function in diabetic retinopathy.

Therefore, we postulated that the coupling between CBF and FCS would be atypical in DR patients compared to healthy individuals. To assess this hypothesis, we gathered resting-state functional magnetic resonance imaging (fMRI) data and arterial spin-labeling (ASL) data from DR patients and age- and sex-matched healthy controls to quantify brain FCS and

CBF. Furthermore, this study examined the classification efficacy of CBF, FCS, and CBF/FCS ratios individually using the SVM method. Understanding the mechanisms underlying neurovascular coupling in diabetic retinopathy is crucial for developing effective therapeutic strategies to preserve vision in individuals affected by this condition.

Methods

Subjects

All participants provided written informed consent. A total of 31 patients with DR, comprising 21 males and 10 females, were recruited from the Department of Ophthalmology at Jiangxi Provincial People's Hospital. The diagnostic criteria for DR patients included fasting plasma glucose levels ≥ 7.0 mmol/L, random plasma glucose levels ≥ 11.1 mmol/L, or a 2-hour glucose level ≥ 11.1 mmol/L. Additionally, patients with nonproliferative DR had characteristics such as microaneurysms, hard exudates, and retinal hemorrhages.

The exclusion criteria for DR patients included the presence of proliferative DR with retinal detachment, vitreous hemorrhage, additional ocular-related complications (such as cataract, glaucoma, high myopia, or optic neuritis), as well as the presence of diabetic nephropathy or diabetic neuropathy.

All HCs fulfilled the criteria, including fasting plasma glucose levels < 7.0 mmol/L, random plasma glucose levels < 11.1 mmol/L, HbA1c levels < 6.5%, absence of ocular diseases (myopia, cataracts, glaucoma, optic neuritis, or retinal degeneration), binocular visual acuity ≥ 1.0 (decimal), no history of ocular surgery, and no mental disorders. Detailed information regarding the subjects is further provided in the study.

Statement of Ethics

The study was carried out in accordance with the principles set forth in the Declaration of Helsinki and received approval from the ethical committee of Jiangxi Provincial People's Hospital. Before participation, all individuals involved in the study provided written informed consent.

Data Acquisition

MRI data were obtained using a 3.0-Tesla MR system (Discovery MR750, General Electric). BOLD and ASL images were captured. Participants were instructed to close their eyes, relax, minimize movements, keep their minds clear, and stay awake throughout the scan. The resting-state perfusion imaging was performed using a pCASL sequence with the following parameters: TR/TE=4699/11 ms; labeling duration=1525 ms; labeling pulse flip angle=18; bandwidth=3.3 kHz/pixel; field of view (FOV) = 240*240; slice thickness= 3.5 mm; no gap. The whole-brain fMRI data was recorded by applying gradient-recalled echo-planar imaging sequence with parameters as follows: TR/TE, 2000 ms/25 ms; gap, 1.2 mm, thickness, 3.0 mm; FOV, 240×240 mm2; acquisition matrix, 64 × 64; 35 axial slices; and flip angle, 90°. The whole scanning time was ~15 min, and a total of 240 volumes of functional images were acquired.

Functional Magnetic Resonance Imaging Data Preprocessing

The fMRI preprocessing was conducted using the Data Processing & Analysis of Brain Imaging (DPABI) toolbox (http://www.rfmri.org/dpabi), which is based on Statistical Parametric Mapping (SPM12) (http://www.fil.ion.ucl.ac.uk) implemented in MATLAB 2013a (MathWorks, Natick, MA, USA). The preprocessing steps involved: 1) removal of the first 10 volumes for each subject, 2) correction for slice timing effects and motion, 3) coregistration of functional and EPI images, normalization of functional images to the Montreal Neurological Institute (MNI) template, and removal of white matter and cerebrospinal fluid signals, and 4) standardization of brain images and band-pass filtering in the range of 0.01–0.08Hz.

Whole-Brain Functional Connectivity Strength Analysis

The BOLD time series data from all voxels within the grey matter were initially extracted. Subsequently, Pearson correlation coefficients were computed for all pairs of grey matter voxels to generate the complete grey matter functional connectivity matrix for each subject. The analysis was confined to positive correlations surpassing a threshold of 0.25 to filter out weak correlations potentially originating from background noise. Voxel connections below the threshold were

adjusted to zero. For a specific voxel x0, the FCS was determined as the mean functional connectivity between x0 and all other voxels. The resultant FCS maps underwent spatial smoothing using a 6 mm × 6 mm × 6 mm Full Width at Half Maximum (FWHM) Gaussian kernel.

CBF Analysis

The CBF images from the control group were first non-linearly normalized to Montreal Neurological Institute (MNI) space and then averaged to create a standard Arterial Spin Labeling (ASL) template. Subsequently, the CBF difference images of each subject underwent non-linear normalization to the standard Echo-Planar Imaging (EPI) template. The CBF images of each subject were then transformed into MNI space utilizing the deformation parameters obtained in the prior step, and resampled to 3 × 3×3 mm cubic voxels. Finally, non-brain tissues were eliminated from the CBF maps, followed by spatial smoothing using a 6 mm Full Width at Half Maximum (FWHM) Gaussian kernel.

Voxel-Wise CBF/FCS Ratio Analyses

To assess the blood supply relative to the connectivity strength, we calculated the CBF/FCS ratio (using original values without z-transformation) for each voxel. Subsequently, the CBF/FCS ratios for each voxel of every subject were transformed into z-scores.

Whole Gray Matter CBF-FCS Coupling Analysis

To quantitatively assess the overall coupling between CBF and FCS, correlation analyses were conducted across voxels for each participant. Subsequently, a two-sample *t*-test was applied to compare the variations in CBF-FCS correlation coefficients between the two groups, with adjustments made for age, sex, and education effects.

Support Vector Machine Analysis

The SVM algorithm was implemented using the Pattern Recognition for Neuroimaging Toolbox (PRoNTo) software. Initially, the classification features included CBF, FCS, and CBF/FCS ratio maps in two groups. Subsequently, the leave-one-out cross-validation (LOOCV) technique was applied in conjunction with the SVM method for classification purposes. The permutation test was utilized to evaluate the overall accuracy of this classification. Total accuracy, specificity, sensitivity, and the area under the receiver operating characteristic curve (AUC) were calculated to evaluate the classification performance of the machine learning model.

The processing flowchart of this study was depicted in Figure 1, illustrating the steps involved such as the calculation of CBF, FCS, and CBF-FCS coupling in patients with diabetic retinopathy compared to healthy controls, as well as the application of machine learning in diabetic retinopathy.

Statistical Analysis

Both the chi-square ($\chi 2$) test and independent-samples *t*-test were utilized to compare clinical variables between the two groups using SPSS version 16.0 (SPSS Inc., Chicago, IL, USA).

One-sample *t*-tests were carried out to evaluate intragroup patterns of zCBF, zFCS, zCBF/FCS ratios maps using SPM8 software.

Additionally, discrepancies in zCBF and zFCS between the two groups at the grey matter voxel level were analyzed using two-sample *t*-tests while controlling for age and sex, with GRF correction implemented at voxel level $p < 0.001$ and cluster level $p < 0.05$.

Two-sample *t*-tests were conducted with age and gender as covariates to investigate between-group disparities in CBF/FCS ratios. Multiple comparisons were adjusted using a voxel-wise Gaussian Random Field (GRF) theory correction method, with significance set at a voxel-wise p-value of < 0.001 and a cluster-wise p-value of < 0.05.

Two-sample *t*-test was applied to compare the variations in CBF-FCS correlation coefficients between the two groups, with adjustments made for age, sex, and education effects.

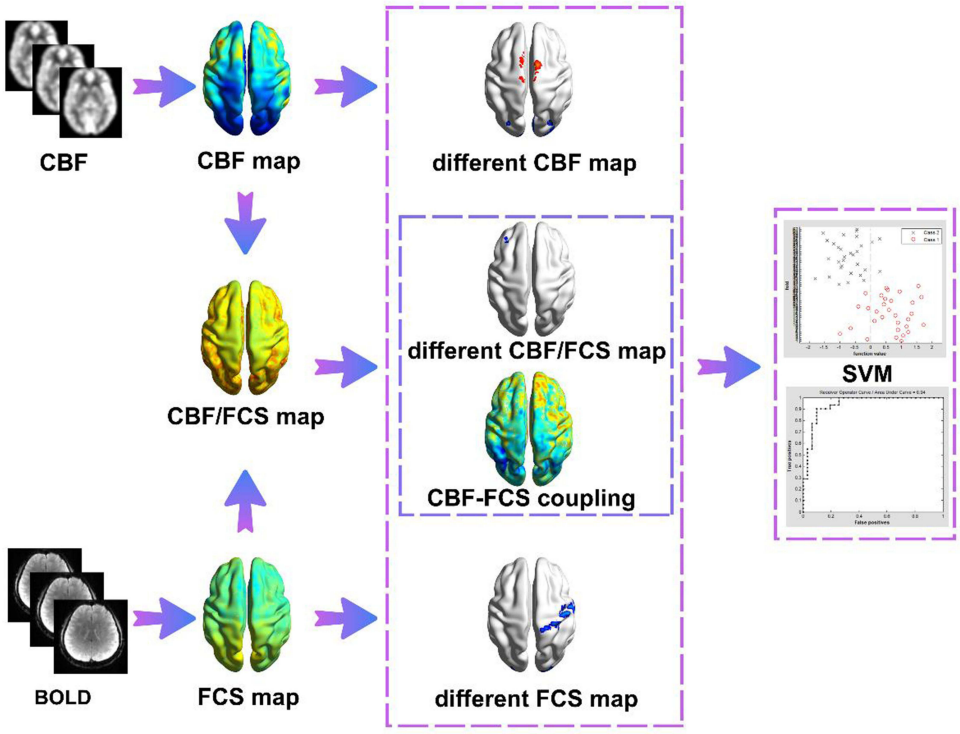

Figure 1 Illustrating the steps involved such as the calculation of CBF, FCS, and CBF-FCS coupling in patients with diabetic retinopathy compared to healthy controlsCalculation of CBF, FCS, CBF-FCS coupling in patients with diabetic retinopathy versus healthy controls, respectively, and for machine learning in diabetic retinopathy. The values of CBF and FCS were first calculated separately by a one-sample *T*-test, and then the two were coupled to calculate the CBF/FCS ratio under the one-sample *T*-test. Then the two-sample *T*-test results for CBF, FCS, and CBF/FCS ratio were calculated separately and for the degree of CBF-FCS coupling within grey matter between the two groups. Finally, the SVM classification of CBF, FCS, and CBF/FCS ratio was calculated for the distinction between DR and HC.
Abbreviations: CBF, cerebral blood flow; FCS, functional connectivity strength; DR, diabetic retinopathy; HC, healthy controls; SVM, support vector machine.

Results

Clinical Features

Age and gender were comparable between the two groups, showing no significant differences ($p > 0.05$) (Table 1).

Spatial Distribution Maps of CBF, FCS, and CBF/FCS Ratio Analysis Between Two Groups

Spatial distribution maps of CBF, FCS, and CBF/FCS ratio were compared between diabetic retinopathy patients and healthy controls. The FCS, CBF, and CBF/FCS ratio maps were standardized to z-scores and averaged within each group. Interestingly,

Table 1 Clinical-Demographic Characteristics of the DR and NC Groups

Condition	DR group	HC group	t	p
Gender (male/female)	21/10	21/10	N/A	N/A
Age (years)	51.16 ± 1.23	52.15± 2.21	−0.216	0.84
BCVA-OD	0.56±0.28	1.10±0.06	−10.35	<0.001*
BCVA-OS	0.53±0.32	1.08±0.54	−9.645	<0.001*
HbA1c (%) Fasting blood	7.34±0.59	N/A	N/A	N/A
Glucose (mmol/L)The	7.97±0.95	N/A	N/A	N/A
Grade of DR	III	N/A	N/A	N/A

Notes: $\chi 2$ test for sex (n). Independent *t*-test for the other normally distributed continuous data (means ± SD). *p<0.001: DR group vs HC group.
Abbreviations: DR, diabetic retinopathy; HC, healthy control; N/A, not applicable; BCVA, best corrected visual acuity; OD, oculus dexter; OS, oculus sinister; DR, diabetic retinopathy; HC, healthy controls.

while the FCS and CBF/FCS ratio mappings showed analogous spatial patterns, the CBF maps exhibited noticeable disparities. The spatial distribution of CBF differed in patients with diabetic retinopathy (Figure 2A) and healthy controls (Figure 2B). The spatial distributions of FCS in diabetic retinopathy patients and healthy controls were represented in Figure 2C and D, respectively. Similarly, the spatial distributions of CBF/FCS ratio in diabetic retinopathy patients and healthy controls were illustrated in Figure 2E and F, respectively.

Different CBF Between Two Groups

Compared to HC, DR patients demonstrated elevated CBF in the bilateral supplementary motor area and decreased CBF in the bilateral lingual gyrus (Figure 3A and Table 2). The mean CBF signal values in the regions of divergence between the two groups are depicted in Figure 3B.

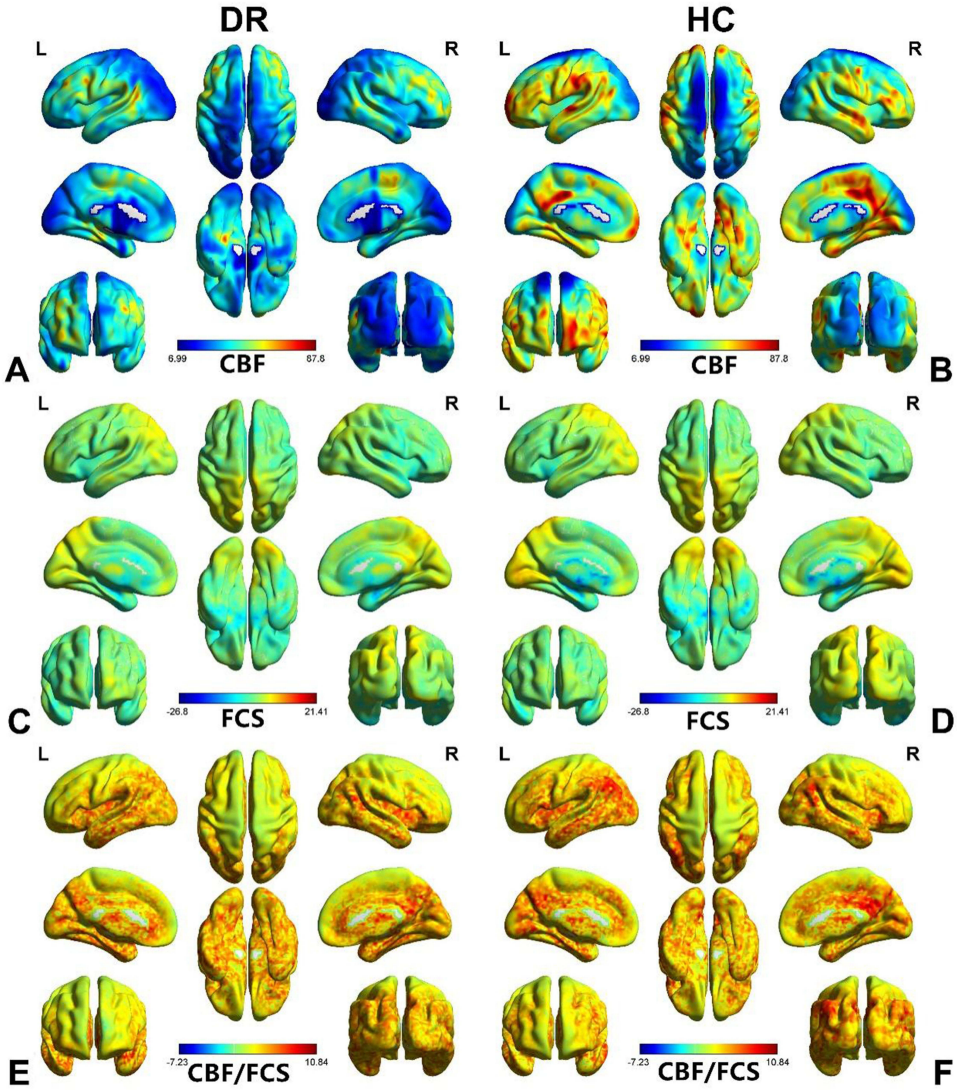

Figure 2 Spatial distribution maps of CBF, FCS, and CBF/FCS ratio in diabetic retinopathy patients and healthy controls. FCS, CBF and CBF/FCS ratio maps were normalized to z-scores. The values were then averaged across subjects within the group. Of these measurements described above, all exhibit similar spatial distributions except for the CBF maps. (**A**) Spatial distribution of CBF in patients with DR. (**B**) Spatial distribution of CBF in healthy controls. (**C**) Spatial distribution of FCS in patients with DR. (**D**) Spatial distribution of FCS in healthy controls. (**E**) Spatial distribution of CBF/FCS ratio in patients with DR. (**F**) Spatial distribution of CBF/FCS ratio in healthy controls. **Abbreviations**: CBF, cerebral blood flow; FCS, functional connectivity strength; DR, diabetic retinopathy; HC, healthy controls; L, left; R, right.

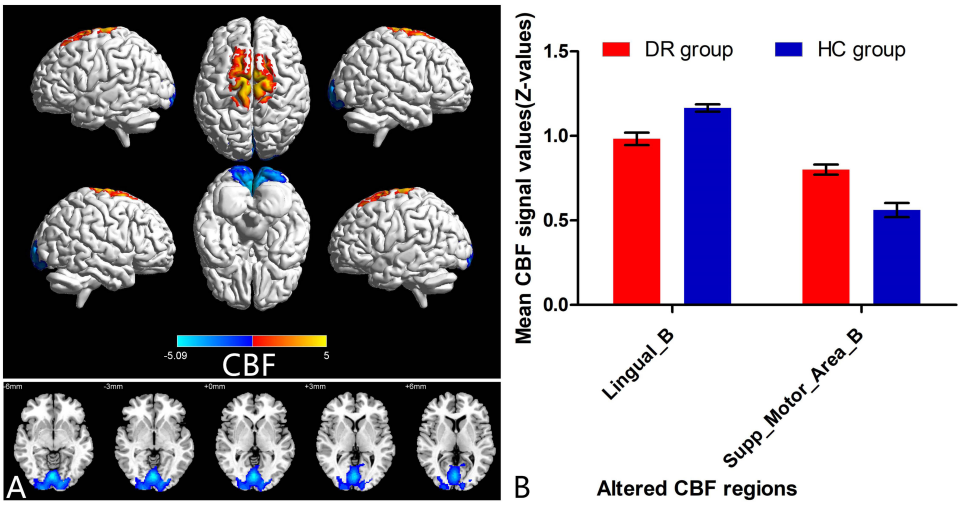

Figure 3 Group differences in CBF between patients with DR and HC (P < 0.05, FDR corrected). (**A**) Spatial distribution of differences in CBF between the two groups. The warm and cold colors indicate increased and decreased CBF in the patients with DR, respectively. (**B**) Mean CBF signal values in regions of differences between the two groups. Compared with HC, DR patients exhibited increased CBF in the Supp_Motor_Area_B and decreased in the Lingual_B.
Abbreviations: CBF, cerebral blood flow; HC, healthy controls; Lingual_B, bilateral lingual gyrus; Supp_Motor_Area_B, bilateral supplementary motor area; SEM, standard error of mean.

Different FCS Between Two Groups

The FCS in DR patients exhibited an increase in the left thalamus and a decrease in the left cerebellum inferior, left lingual gyrus, right middle occipital gyrus, and right central posterior gyrus (Figure 4A and Table 3). The average FCS signal values in the areas of divergence between the two groups are illustrated in Figure 4B.

Different CBF-FCS Ratio Between Two Groups

The cerebral blood flow to functional connectivity strength (CBF/FCS) ratio in DRpatients revealed an elevated CBF/FCS ratio in the right calcarine fissure and surrounding cortex and a decreased ratio in the left middle frontal gyrus (Figure 5A and Table 4). The average CBF/FCS ratio signal values in the areas of divergence between the two groups are shown in Figure 5B.

CBF-FCS Coupling Between Two Groups

Significant across-voxel correlations between cerebral blood flow (CBF) and functional connectivity strength (FCS) were observed in every participant, encompassing both diabetic retinopathy patients and healthy controls (Figure 6A). Nevertheless, the correlations in patients with diabetic retinopathy exhibited slightly lower values compared to those in healthy controls (Figure 6B).

Table 2 Group Difference in CBF Between DR and HC

Region	Side	MNI coordinate			Voxel	t value
		x	y	z		
Lingual	R	2	−78	−4	4924	−5.0873
Supp_Motor_Area	L	−2	−12	74	2071	4.9987

Notes: GRF correction implemented at voxel level p < 0.001 and cluster level p < 0.05.
Abbreviations: Lingual_B, bilateral lingual gyrus; Supp_Motor_Area_B, bilateral supplementary motor area; CBF, cerebral blood flow; DR, diabetic retinopathy; HC, healthy controls.

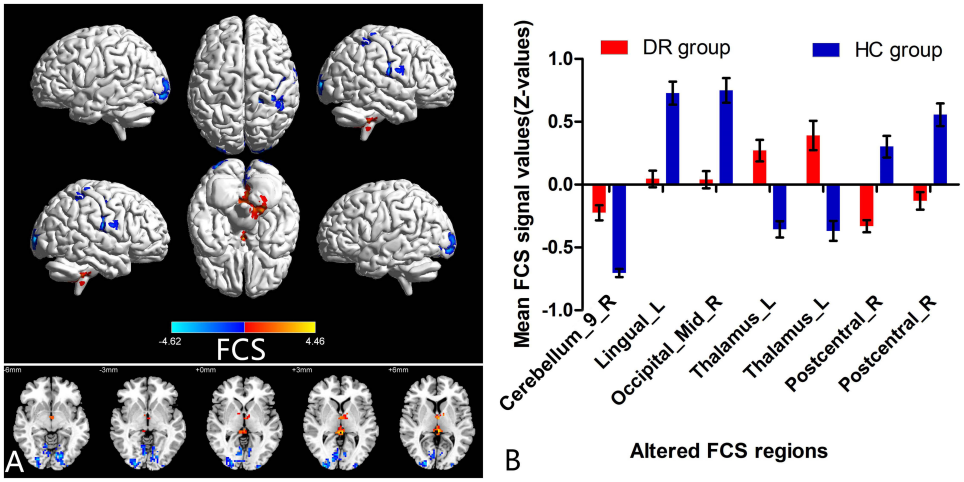

Figure 4 Group differences in FCS between patients with DR and HC (P < 0.05, FDR corrected). (**A**) Spatial distribution of differences in FCS between the two groups. The warm and cold colors indicate increased and decreased FCS in the patients with DR, respectively. (**B**) Mean FCS signal values in regions of differences between the two groups. Compared with HC, DR patients exhibited increased FCS in the Thalamus_L and decreased in the Cerebellum_9_R, Lingual_L, Occipital_Mid_R and Postcentral_R. **Abbreviations**: FCS, functional connectivity strength; HC, healthy controls; Thalamus_L, left thalamus; Cerebellum_9_R, left cerebellum inferior; Lingual_L, left lingual gyrus; Occipital_Mid_R, right middle occipital gyrus; Postcentral_R, right central posterior gyrus; SEM, standard error of mean.

SVM Classification Results

The SVM classification utilizing CBF achieved an overall accuracy of 85.48% and the SVM classifier exhibited an ROC curve with an area under the curve (AUC) of 0.94 (Figure 7A). In contrast, the SVM classification based on FCS resulted in an accuracy of 64.52%, with the AUC of the SVM classifier at 0.75 (Figure 7B). Furthermore, the SVM classification utilizing the CBF/FCS ratio attained a total accuracy of 37.10%, with the AUC of the SVM classifier reaching 0.39 (Figure 7C).

Discussion

To the best of our knowledge, this study represents the initial attempt to integrate ASL and BOLD techniques to assess CBF-FCS coupling in diabetic retinopathy. The examination revealed a slight reduction in whole grey matter CBF-FCS coupling in the diabetic retinopathy (DR) group when compared to healthy controls. Additionally, CBF-FCS coupling decreased in motor areas and increased in visual areas within the DR group. These outcomes contribute to a deeper comprehension of the neural mechanisms implicated in diabetic retinopathy through the lens of neurovascular coupling.

Table 3 Group Difference in FCS Between DR and HC

Region	Side	MNI Coordinate			Voxel	t value
		x	y	z		
Cerebellum_9	R	6	−48	−33	156	4.3289
Lingual	L	−18	−81	−6	157	−4.3781
Occipital_Mid	R	24	−93	6	218	−4.6250
Thalamus_1	L	3	−6	9	74	4.0255
Thalamus_2	L	−3	−33	6	55	4.4628
Postcentral_1	R	60	−12	18	71	−4.0638
Postcentral_2	R	30	−33	51	118	−3.9989

Note: GRF correction implemented at voxel level p < 0.001 and cluster level p < 0.05.

Abbreviations: Thalamus_L, left thalamus; Cerebellum_9_R, left cerebellum_9; Lingual_L, left lingual gyrus; Occipital_Mid_R, right middle occipital gyrus; Postcentral_R, right postcentral gyrus.FCS, functional connectivity strength; DR, diabetic retinopathy; HC, healthy controls;

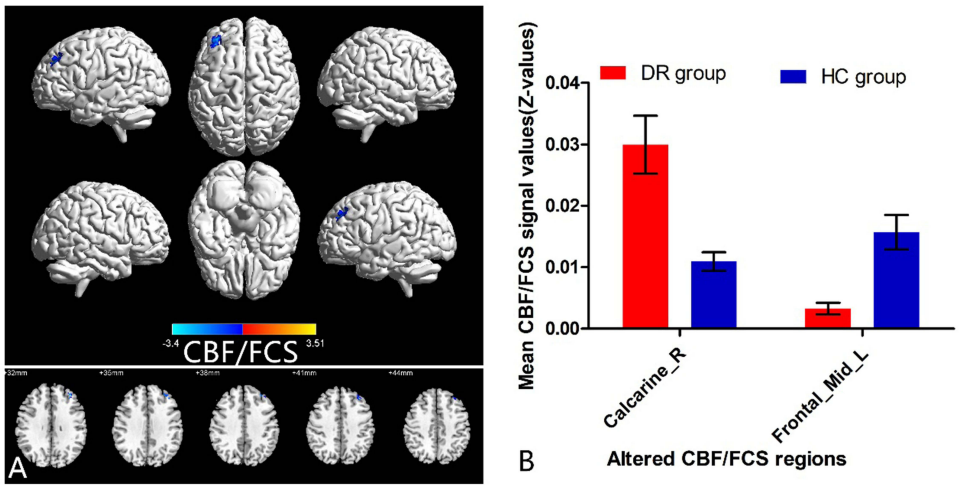

Figure 5 Group differences in CBF/FCS ratio between patients with DR and HC ($P < 0.05$, FDR corrected). (**A**) Spatial distribution of differences in CBF/FCS ratio between the two groups. The warm and cold colors indicate increased and decreased CBF/FCS ratio in the patients with DR, respectively. (**B**) Mean CBF/FCS signal values in regions of differences between the two groups. Compared with HC, DR patients exhibited increased CBF/FCS ratio in the Calcarine_R and decreased in the Frontal_Mid_L.
Abbreviations: CBF, cerebral blood flow; FCS, functional connectivity strength; HC, healthy controls; Calcarine_R, right calcarine fissure and surrounding cortex; Frontal_Mid_L, left middle frontal gyrus; SEM, standard error of mean.

Our findings revealed increased CBF in the bilateral supplementary motor area of DR patients, whereas decreased CBF was observed in the bilateral lingual gyrus. The supplementary motor area (SMA) is widely recognized for its involvement in motor function.[28] The supplementary motor area (SMA) primarily governs internally generated movements, as opposed to those initiated in response to external stimuli. It plays a key role in the control of movements, including finger movements. In individuals with type 2 diabetes mellitus, elevated activity is observed in the right supplementary motor area.[29,30] In type 1 diabetes mellitus, early neuroretinal dysfunction is linked to the loss of peripheral motor units.[31])The loss of peripheral motor units can trigger functional reorganization within the supplementary motor area, potentially causing increased cerebral blood flow perfusion in the bilateral supplementary motor area. This elevation observed in diabetic retinopathy (DR) patients aligns with findings from previous studies.[15]

The lingual gyrus plays a primary role in visual processing, particularly in the context of letters, and it may also contribute to logical analysis and the processing of visual memory.[32] The precise reason for the diminished cerebral blood flow perfusion in the bilateral lingual gyrus among DR patients is not definitively established, but it could be associated with a decrease in the volume of the lingual gyrus. A study evaluating gray matter volume alterations in individuals with type 1 diabetes mellitus using seed-based d mapping software indicated a reduction in gray matter volume specifically in the right lingual gyrus.[33] Decreased cerebral blood flow perfusion to the lingual gyrus in diabetic patients could potentially result in a reduction in gray matter volume within this brain region. Additionally, a separate study demonstrated a selective correlation between the thickness of the lower limit of the Retinal Nerve Fiber Layer

Table 4 Group Difference in CBF/FCS Between DR and HC

Region	Side	MNI Coordinate			Voxel	t value
		x	y	z		
Calcarine	R	18	−72	8	28	3.5135
Frontal_Mid	L	−36	42	32	72	−3.4005

Note: GRF correction implemented at voxel level $p < 0.001$ and cluster level $p < 0.05$.
Abbreviations: Calcarine_R, right calcarine fissure and surrounding cortex; Frontal_Mid_L, left middle frontal gyrus; CBF, cerebral blood flow;.FCS, functional connectivity strength; DR, diabetic retinopathy; HC, healthy controls;

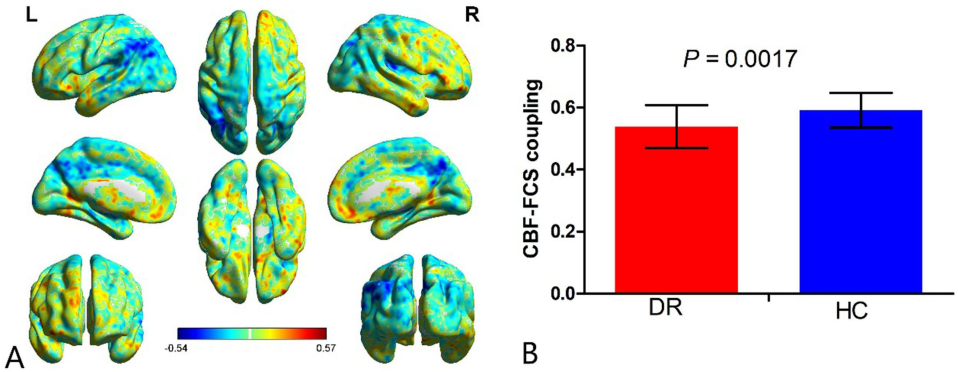

Figure 6 Mean CBF-FCS coupling across patients in DR patients. (**A**) Spatial images of the mean CBF-FCS coupling. (**B**) Group comparison of CBF-FCS coupling between DR patients and healthy controls. The right histogram shows that the degree of CBF-FCS coupling is slightly lower in DR patients than in healthy controls.
Abbreviations: CBF, cerebral blood flow; FCS, functional connectivity strength; HC, healthy controls; std, standard deviation.

(RNFL) in older adults without dementia and the substructure volume of the lingual gyrus.[34] The thickness of the Retinal Nerve Fiber Layer (RNFL) is linked to unmyelinated axons from retinal ganglion cells, neuroglial cells, and retinal blood vessels. One of the most notable clinicopathological features of DRis a surge in retinal neovascularization.[35] Hence, heightened retinal vascularization could contribute to thickening of the retinal nerve fiber layer (RNFL). Conversely, compromised cerebral blood flow and perfusion in individuals with DR might potentially result in a decrease in the size of the lingual gyrus in non-demented elderly individuals.

In DR patients, compared to healthy controls, FCS values demonstrated an increase in the left thalamus and decreases in the left cerebellum inferior, left lingual gyrus, right middle occipital gyrus, and right central posterior gyrus. The thalamus serves as a central hub for sensory processing, where all senses except olfaction converge before relaying information to the cerebral cortex, including visual inputs. FCS characterizes the brain-wide functional connectivity of each voxel within the global network, offering insight into the information exchange dynamics throughout the brain network.[19] Hence, the heightened FCS observed in the left thalamus suggests an augmentation in information transfer within the entire brain network. This finding contrasts with prior studies.[20] In the current study, an increased FCS was observed in the left thalamus. Although the precise mechanism remains unclear, prior research suggests that heightened functional connectivity in individuals with type 2 diabetes mellitus may signify a compensatory mechanism in response to brain volume reduction starting from the pre-diabetes stage.[36] Hence, it is plausible that the heightened FCS observed in the left thalamus serves as a compensatory mechanism following visual impairment in patients with DR.

The cerebellum plays a crucial role in body muscle tension, muscle tone, and various functions associated with body movement. Diabetic retinopathy stands as the predominant microvascular complication of diabetes. Prior research indicates that individuals with type 2 diabetes and microvascular complications may manifest disruptions in nodal properties within the occipital visual network, cerebellum, and middle temporal gyrus.[37] Studies have revealed reduced grey matter volumes in the right lingual gyrus, cerebellum, precuneus gyrus, left inferior temporal gyrus, and middle temporal gyrus in individuals with type 1 diabetes.[33] Studies have indicated that structural brain volumes are decreased in regions such as the prefrontal cortex, hippocampus, amygdala, insula, cingulate cortex, cerebellum, caudate nucleus, basal forebrain, and thalamus in individuals with type 2 diabetes.[38] The decrease in FCS has been linked to the compromised functional connectivity of this area. We propose that the decline in cerebellar grey matter volume significantly contributes to the decreased FCS observed. Both the lingual gyrus and middle occipital gyrus are situated in the occipital lobe, which serves as the hub of the visual cortex and is intricately connected to the visual network. These observations align with our earlier research findings.[20] In diabetic retinopathy (DR) patients, the visual network exhibits diminished intra-network FCS. The postcentral gyrus, responsible for processing sensory information linked to somato-sensation, resides within the sensorimotor network (SMN) and holds a pivotal role therein. Our prior research unveiled abnormal functional connections among the visual network (VN), default mode network (DMN), salience network (SN), and sensorimotor network in individuals with DR.[39] Another study demonstrated that interhemispheric coordination

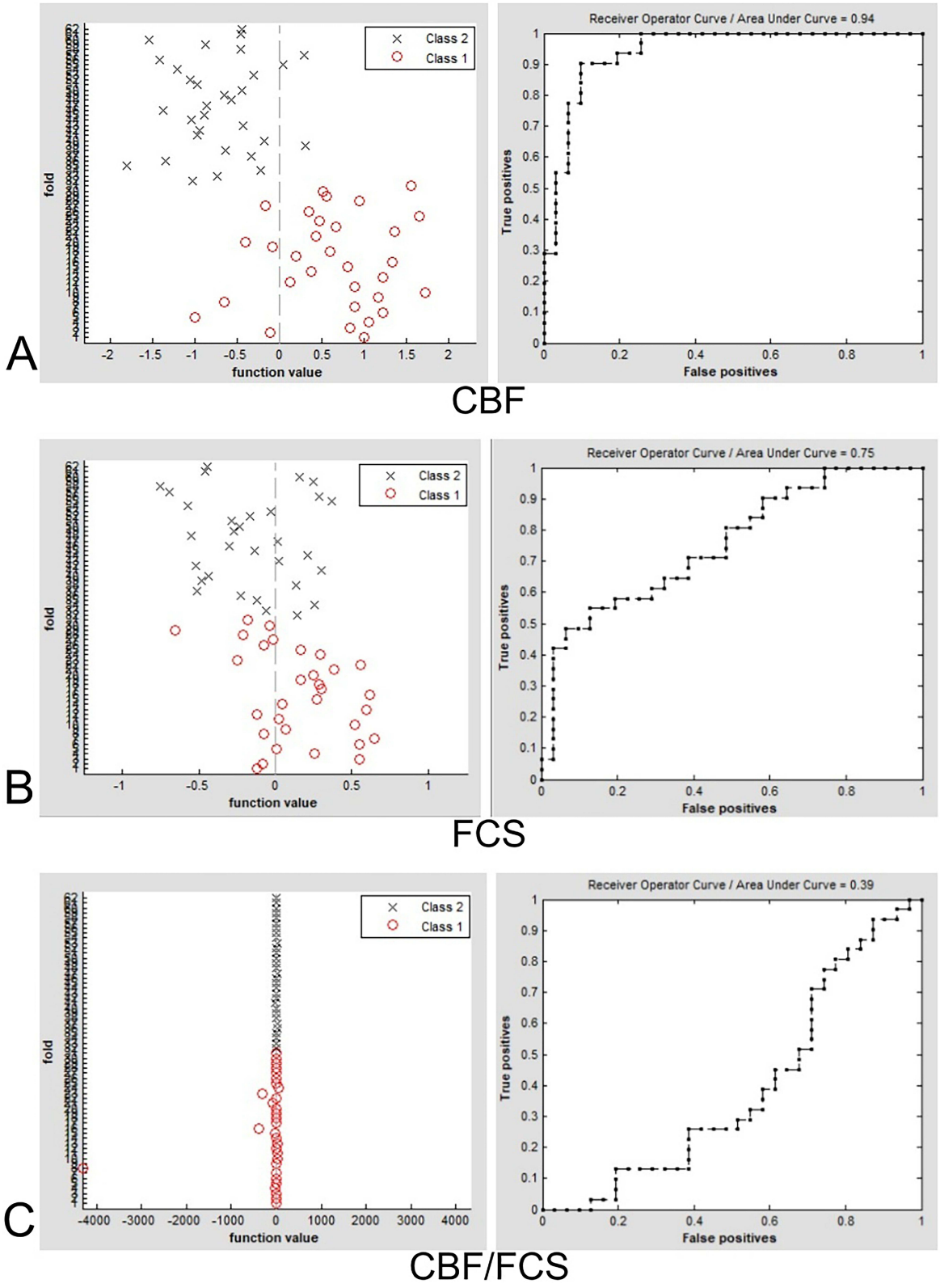

Figure 7 Classification results of SVM for DR patients and healthy controls. (**A**) SVM classification results based on CBF values. (**B**) SVM classification results based on FCS values. (**C**) SVM classification results based on CBF/FCS ratio. The left column of images shows a 10-fold in the class 1 (DR group) and class 2 (HC group). The right column shows the ROC curve of the SVM classifier with AUC values of 0.94, 0.75, and 0.39, respectively.

Abbreviations: CBF, cerebral blood flow; FCS, functional connectivity strength; HC, healthy controls; SVM, support vector machine.

among the auditory network, visual network, default mode network, and sensorimotor network is significantly compromised in patients with diabetic retinopathy.[40]

Neurovascular coupling relies on the integrity of neurovascular units, encompassing neurons, glial cells, and vascular components.[41] Patients with DR show a decreased CBF/FCS ratio compared to healthy individuals, suggesting the presence of neurovascular decoupling.[42] One possible explanation is that astrocytes may be impaired in DR patients, leading to a decreased CBF/FCS ratio. Astrocytes in the brain play a crucial role as intermediaries connecting neural activity to the vascular response.[43,44] The aberrant astrocytes in the basal ganglion could stem from astrocyte damage. This abnormality may disrupt the link between neural activity and vascular response, leading to reduced CBF in the region and thus lower CBF-FCS values. Another potential scenario is that increased plasma glutamate levels in individuals with diabetic retinopathy can cause constriction of small arterial smooth muscle in the brain. In a recent study, it has been demonstrated that the axons of specific glutamatergic neurons induce dilation in the small arteries they innervate through synaptic-like transmission occurring at the connections between nerve terminals and small arterial smooth muscle cells (aSMCs).[45] Studies have indicated that glutamate and glutamine hold promise as potential biomarkers for diabetic retinopathy.[46] This finding presents a new avenue for exploring the relationship between DR and cerebral blood flow–functional connectivity strength (CBF-FCS) coupling. Individuals with DR exhibited a diminished CBF/FCS ratio in the left middle frontal gyrus, aligning with the reduced CBF-FCS coupling observed in the overall gray matter. Notably, the posterior segment of the middle frontal gyrus houses the cortical lateral visual center, responsible for controlling eye movements, head rotations, and neck movements, along with housing the premotor and supplementary motor areas (SMA). Curiously, elevated CBF/FCS ratios were observed in the right calcarine fissure and surrounding cortex in the DR group, contrary to expectations. The primary visual cortex, encompassing the calcarine fissure and neighboring cortical regions, processes visual stimuli originating from the lateral geniculate body and constitutes a vital component of the visual network. The heightened CBF-FCS correlation in these regions may reflect enhanced synchrony between cerebral blood flow and functional connectivity among DR patients, potentially influenced by compensatory mechanisms.

In our investigation, we employed CBF, fFCS, and the CBF/FCS ratio as distinct features. Unfortunately, only the SVM classification based on CBF achieved a notable total accuracy of 85.48% and an area under the curve (AUC) value of 0.94 on the receiver operating characteristic (ROC) curve. Conversely, the FCS and CBF/FCS ratios yielded lower total accuracies of 64.52% and 37.10%, with respective AUC values of 0.75 and 0.39. These results suggest that CBF might serve as a more sensitive biomarker in distinguishing individuals with diabetic retinopathy from healthy controls.

Limitations

In this investigation, we utilized CBFand FCS to explore neurovascular coupling in individuals with diabetic retinopathy. Despite the valuable insights gained from this study, there are several limitations to acknowledge. Firstly, ensuring result reproducibility over time is crucial, necessitating the collection of a larger dataset to validate our current findings. Secondly, numerous studies have linked neuroimaging outcomes with clinical metrics, which can potentially serve as neuroimaging markers for certain neurological disorders. Regrettably, we did not gather cognitive behavior and clinical parameters in the present study, highlighting the need for future research to investigate the correlation between functional network deficits and clinical implications. Lastly, the adoption of a standard gray mask for the neurovascular coupling analysis overlooked the issue of incomplete coverage in individual image acquisition. Subsequently, future studies should employ a common group-level mask for both resting fMRI and ASL to carry out comprehensive CBF–FCS coupling analysis. In the future research, We will conduct correlation analysis between clinical scales and neurovascular coupling changes in patients with DR to investigate the neural mechanisms underlying cognitive dysfunction in DR. Additionally, we plan to increase the sample size and perform repeated assessments of abnormal neurovascular coupling changes in DR patients to enhance the robustness of our findings. Furthermore, this study integrates non-invasive neuromodulation techniques such as transcranial magnetic stimulation (TMS) and cognitive behavioral therapy to enhance neurovascular coupling function in DR patients, aiming for potential clinical advancements.

Conclusion

In conclusion, our study observed an increased CBF/FCS ratio in brain regions associated with vision-related functions and a decreased CBF/FCS ratio in areas linked to motor-related processes. An elevated CBF/FCS ratio suggests that patients with DR may have a reduced volume of gray matter in the brain. A decrease in its ratio indicates a decrease in regional CBF in patients with DR. These results propose that neurovascular decoupling in the brain may represent a significant neural mechanism implicated in the pathophysiology of diabetic retinopathy. Understanding the mechanisms underlying neurovascular coupling in diabetic retinopathy is crucial for developing effective therapeutic strategies to preserve vision in individuals affected by this condition.

Data Sharing Statement

The raw data supporting the conclusions of this article will be made available. Further inquiries can be directly to the corresponding author.

Acknowledgments

We acknowledge the assistance provided by the Natural Science Foundation of Jiangxi Province (20212BAB216058), Jiangxi Provincial Health Technology Project (202210012, 202310114 and 202410008), and Jiangxi Provincial traditional Chinese Technology Project (2022B840 and 2023A0138).

Disclosure

The authors declare that they have no conflict of interest with regard to this work.

References

1. Wong TY, Cheung CMG, Larsen M, Sharma S, Simó R. Diabetic retinopathy. *Nat Rev Dis Primer*. 2016;2:16012.
2. Wolfensberger TJ, Hamilton AM. Diabetic retinopathy--an historical review. *Semin Ophthalmol*. 2001;16(1):2–7. doi:10.1076/soph.16.1.2.4220
3. Teo ZL, Tham YC, Yu M, et al. Global prevalence of diabetic retinopathy and projection of burden through 2045: systematic review and meta-analysis. *Ophthalmology*. 2021;128(11):1580–1591. doi:10.1016/j.ophtha.2021.04.027
4. Duong TQ. Magnetic resonance imaging of the retina: from mice to men. *Magn Reson Med*. 2014;71(4):1526–1530. doi:10.1002/mrm.24797
5. Yu Y, Yan LF, Sun Q, et al. Neurovascular decoupling in type 2 diabetes mellitus without mild cognitive impairment: potential biomarker for early cognitive impairment. *NeuroImage*. 2019;200:644–658. doi:10.1016/j.neuroimage.2019.06.058
6. Messier C, Tsiakas M, Gagnon M, Desrochers A, Awad N. Effect of age and glucoregulation on cognitive performance. *Neurobiol Aging*. 2003;24 (7):985–1003. doi:10.1016/S0197-4580(03)00004-6
7. Little K, Llorián-Salvador M, Scullion S, et al. Common pathways in dementia and diabetic retinopathy: understanding the mechanisms of diabetes-related cognitive decline. *Trends Endocrinol Metab TEM*. 2022;33(1):50–71. doi:10.1016/j.tem.2021.10.008
8. Busiguina S, Fernandez AM, Barrios V, et al. Neurodegeneration is associated to changes in serum insulin-like growth factors. *Neurobiol Dis*. 2000;7(6):657–665. doi:10.1006/nbdi.2000.0311
9. Vaishnavi SN, Vlassenko AG, Rundle MM, Snyder AZ, Mintun MA, Raichle ME. Regional aerobic glycolysis in the human brain. *Proc Natl Acad Sci U S A*. 2010;107(41):17757–17762. doi:10.1073/pnas.1010459107
10. Li J, Chen P, Bao Y, Sun Y, He J, Liu X. PET imaging of vesicular monoamine transporter 2 in early diabetic retinopathy using [18F]FP-(+)-DTBZ. *Mol Imaging Biol*. 2020;22(5):1161–1169. doi:10.1007/s11307-019-01443-1
11. Hernández C, Candell-Riera J, Ciudin A, Francisco G, Aguadé-Bruix S, Simó R. Prevalence and risk factors accounting for true silent myocardial ischemia: a pilot case-control study comparing type 2 diabetic with non-diabetic control subjects. *Cardiovasc Diabetol*. 2011;10:9. doi:10.1186/1475-2840-10-9
12. Roberts DA, Rizi R, Lenkinski RE, Leigh JS. Magnetic resonance imaging of the brain: blood partition coefficient for water: application to spin-tagging measurement of perfusion. *J Magn Reson Imaging JMRI*. 1996;6(2):363–366. doi:10.1002/jmri.1880060217
13. Haller S, Zaharchuk G, Thomas DL, Lovblad KO, Barkhof F, Golay X. Arterial spin labeling perfusion of the brain: emerging clinical applications. *Radiology*. 2016;281(2):337–356. doi:10.1148/radiol.2016150789
14. Ilik İ, Arslan H, Yokuş A, Batur M, Üçler R, Akdeniz H. Cerebral perfusion in type 2 diabetes mellitus: a preliminary study with MR perfusion. *Clin Neurol Neurosurg*. 2023;231:107816. doi:10.1016/j.clineuro.2023.107816
15. Huang X, Wen Z, Tong Y, Qi CX, Shen Y. Altered resting cerebral blood flow specific to patients with diabetic retinopathy revealed by arterial spin labeling perfusion magnetic resonance imaging. *Acta Radiol*. 2021;62(4):524–532. doi:10.1177/0284185120932391
16. Biswal B, Yetkin FZ, Haughton VM, Hyde JS. Functional connectivity in the motor cortex of resting human brain using echo-planar MRI. *Magn Reson Med*. 1995;34(4):537–541. doi:10.1002/mrm.1910340409
17. Biswal BB. Resting state fMRI: a personal history. *NeuroImage*. 2012;62(2):938–944. doi:10.1016/j.neuroimage.2012.01.090
18. Nair A, Keown CL, Datko M, Shih P, Keehn B, Müller RA. Impact of methodological variables on functional connectivity findings in autism spectrum disorders. *Hum Brain Mapp*. 2014;35(8):4035–4048. doi:10.1002/hbm.22456
19. Liang X, Zou Q, He Y, Yang Y. Coupling of functional connectivity and regional cerebral blood flow reveals a physiological basis for network hubs of the human brain. *Proc Natl Acad Sci*. 2013;110(5):1929–1934. doi:10.1073/pnas.1214900110

20. Huang X, Tong Y, Qi CX, Dan HD, Deng QQ, Shen Y. Large-scale neuronal network dysfunction in diabetic retinopathy. *Neural Plast*. 2020;2020:1–13.
21. Raichle ME, Gusnard DA. Appraising the brain's energy budget. *Proc Natl Acad Sci U S A*. 2002;99(16):10237–10239. doi:10.1073/pnas.172399499
22. Raichle ME, Mintun MA. Brain work and brain imaging. *Annu Rev Neurosci*. 2006;29:449–476. doi:10.1146/annurev.neuro.29.051605.112819
23. Kuschinsky W. Coupling of function, metabolism, and blood flow in the brain. *Neurosurg Rev*. 1991;14(3):163–168. doi:10.1007/BF00310651
24. Venkat P, Chopp M, Chen J. New insights into coupling and uncoupling of cerebral blood flow and metabolism in the brain. *Croat Med J*. 2016;57(3):223–228. doi:10.3325/cmj.2016.57.223
25. Zhu J, Zhuo C, Xu L, Liu F, Qin W, Yu C. Altered coupling between resting-state cerebral blood flow and functional connectivity in schizophrenia. *Schizophr Bull*. 2017;43(6):1363–1374. doi:10.1093/schbul/sbx051
26. Ruan Z, Sun D, Zhou X, et al. Altered neurovascular coupling in patients with vascular cognitive impairment: a combined ASL-fMRI analysis. *Front Aging Neurosci*. 2023;15:1224525. doi:10.3389/fnagi.2023.1224525
27. Shang S, Ye J, Wu J, et al. Early disturbance of dynamic synchronization and neurovascular coupling in cognitively normal Parkinson's disease. *J Cereb Blood Flow Metab*. 2022;42(9):1719–1731. doi:10.1177/0271678X221098503
28. Hertrich I, Dietrich S, Ackermann H. The role of the supplementary motor area for speech and language processing. *Neurosci Biobehav Rev*. 2016;68:602–610. doi:10.1016/j.neubiorev.2016.06.030
29. Xie H, Yu Y, Yang Y, et al. Commonalities and distinctions between the type 2 diabetes mellitus and Alzheimer's disease: a systematic review and multimodal neuroimaging meta-analysis. *Front Neurosci*. 2023;17:1301778. doi:10.3389/fnins.2023.1301778
30. Liu J, Yang X, Li Y, Xu H, Ren J, Zhou P. Cerebral blood flow alterations in type 2 diabetes mellitus: a systematic review and meta-analysis of arterial spin labeling studies. *Front Aging Neurosci*. 2022;14:847218. doi:10.3389/fnagi.2022.847218
31. Picconi F, Mataluni G, Ziccardi L, et al. Association between early neuroretinal dysfunction and peripheral motor unit loss in patients with type 1 diabetes mellitus. *J Diabetes Res*. 2018;2018:1–9. doi:10.1155/2018/9763507
32. Palejwala AH, Dadario NB, Young IM, et al. Anatomy and white matter connections of the lingual gyrus and cuneus. *World Neurosurg*. 2021;151:e426–37. doi:10.1016/j.wneu.2021.04.050
33. Liu J, Fan W, Jia Y, et al. Altered gray matter volume in patients with type 1 diabetes mellitus. *Front Endocrinol*. 2020;11:45. doi:10.3389/fendo.2020.00045
34. Shi Z, Cao X, Hu J, et al. Retinal nerve fiber layer thickness is associated with hippocampus and lingual gyrus volumes in nondemented older adults. *Prog Neuropsychopharmacol Biol Psychiatry*. 2020;99:109824. doi:10.1016/j.pnpbp.2019.109824
35. Tang L, Xu GT, Zhang JF. Inflammation in diabetic retinopathy: possible roles in pathogenesis and potential implications for therapy. *Neural Regen Res*. 2023;18(5):976–982. doi:10.4103/1673-5374.355743
36. Jing J, Liu C, Zhu W, et al. Increased resting-state functional connectivity as a compensatory mechanism for reduced brain volume in prediabetes and type 2 diabetes. *Diabetes Care*. 2023;46(4):819–827. doi:10.2337/dc22-1998
37. Zhang D, Huang Y, Gao J, et al. Altered functional topological organization in type-2 diabetes mellitus with and without microvascular complications. *Front Neurosci*. 2021;15:726350. doi:10.3389/fnins.2021.726350
38. Roy B, Ehlert L, Mullur R, et al. Regional brain gray matter changes in patients with type 2 diabetes mellitus. *Sci Rep*. 2020;10(1):9925. doi:10.1038/s41598-020-67022-5
39. Huang X, Tong Y, Qi CX, Xu YT, Dan HD, Shen Y. Disrupted topological organization of human brain connectome in diabetic retinopathy patients. *Neuropsychiatr Dis Treat*. 2019;15:2487–2502. doi:10.2147/NDT.S214325
40. Wan S, Xia WQ, Zhong YL. Aberrant interhemispheric functional connectivity in diabetic retinopathy patients. *Front Neurosci*. 2021;15:792264. doi:10.3389/fnins.2021.792264
41. Hawkins BT, Davis TP. The blood-brain barrier/neurovascular unit in health and disease. *Pharmacol Rev*. 2005;57(2):173–185. doi:10.1124/pr.57.2.4
42. Chen Y, Cui Q, Sheng W, et al. Anomalous neurovascular coupling in patients with generalized anxiety disorder evaluated by combining cerebral blood flow and functional connectivity strength. *Prog Neuropsychopharmacol Biol Psychiatry*. 2021;111:110379. doi:10.1016/j.pnpbp.2021.110379
43. Stobart JL, Anderson CM. Multifunctional role of astrocytes as gatekeepers of neuronal energy supply. *Front Cell Neurosci*. 2013;7:38. doi:10.3389/fncel.2013.00038
44. Howarth C. The contribution of astrocytes to the regulation of cerebral blood flow. *Front Neurosci*. 2014;8:103. doi:10.3389/fnins.2014.00103
45. Zhang D, Ruan J, Peng S, et al. Synaptic-like transmission between neural axons and arteriolar smooth muscle cells drives cerebral neurovascular coupling. *Nat Neurosci*. 2024;27:232–248. doi:10.1038/s41593-023-01515-0
46. Rhee SY, Jung ES, Park HM, et al. Plasma glutamine and glutamic acid are potential biomarkers for predicting diabetic retinopathy. *Metabolomics off J Metabolomic Soc*. 2018;14(7):89.